DESIGN AND EXPERIMENT OF AUTOMATIC SEED FILLING DEVICE FOR SOYBEAN PLOT SEEDER

1

大豆小区播种机自动供种装置设计与试验

Sheng WANG*1), Yuanyuan LIU1), Zhonghua SHI1)

Zhengzhou Vocational College of Information Technology Henan / China Corresponding author: Sheng Wang Tel: 18613718234; E-mail: lyy9485@163.com DOI: https://doi.org/10.35633/inmateh-77-06

Keywords: soybean; automatic seed filling; simulation; field experiment

ABSTRACT

To address problems such as low working efficiency and the difficulty of manual seed filling during seed breeding with a soybean plot seeder, a new type of automatic seed filling device with a rotational disc was designed. The design integrates a rotational seed disc coupled with seed cups. The automatic seed filling device consists of a mechanical part and an electrical control part. The mechanical part includes seed cups, a seed plate, a base, and a mounting bracket, while the electrical control part includes a PLC, motor, and driver. By analysing the soybean seed delivery process, the factors influencing the design of the seed cup structure were identified, and key structural design and parameter analysis of the seed cup were conducted. Field test results showed that the minimum qualification rate of seed cup offset was 98.78%, and the minimum qualification rate of seed filling without seed breakage was 96.18%. These results demonstrate good accuracy and reliability, meeting the agronomic requirements of field seeding with plot seeders, and the experimental performance reached the design expectations.

摘要

针对现有小区大豆播种机田间育种试验过程中,需要人工频繁更换不同品种种子,换种效率低的问题,研究设计一种新型的自动转盘式小区大豆播种机自动供种装置。整个供种装置采用转盘式的圆形种盘与种杯组合的方式,使用 PLC 控制工作过程,完成小区大豆播种机播种过程中的自动换种。该自动供种装置包括机械部分和电控部分,其中机械部分由种杯、种盘、底座、安装支架等组成。电控部分由 PLC、电机、驱动器等组成。通过对大豆种子送种作业过程分析,得到影响种杯结构设计的因素,开展了种杯关键结构的设计与参数分析。田间试验结果表明: 种杯的偏移量合格率最小为98.78%,种子无破碎供种合格率最小为96.18%,具有较好的准确性和可靠性,符合小区播种机上种的实际田间农艺要求,试验效果达到设计要求。

INTRODUCTION

With the rapid development of agriculture breeding technology in China, the holistic size and standardization of the trial plot breeding are increasing simultaneously. However, the research and development of the relative breeding machinery device is still relatively outmoded. For a long period, the trail plot seeding in China adopt the traditional handmade style. The laborious, complex processes, low seeing efficiency and un equilibrium quality affect the accuracy and scientific of the trail plot research (*Zhu et al., 2015; Huang et al., 2018; Dai et al., 2012*). In contrast, the plot seeder can maintain high working efficiency, congruity of seeding standard and avoid the obvious experimental error made by operators. It is well accepted that the plot seeders, a specialized seeder for breeding research, can breed new seed species, carry out the comparative tests in different seeds (*Dai et al., 2012; Kroulík et al., 2016; Liu et al., 2020*). For the specialized agricultural machine device, the main standard of the plot seed includes seeding accurate quantitative seeds in the defined area plot, seeding different type seeds in different plots preciously and cleaning-filling seeds conveniently (*Liu et al., 2020; Yang et al., 2019; Panigrahi et al., 2021; Yang et al., 2019; Ghafori et al., 2011*).

For the purpose of meeting the breeding requirements, there are three main type plot seeders include the plot precision seeder, the plot drill seeder and the plot plant row seeders. Their main structure includes the filing module, the cleaning module, the seeding module, the mulch suppression module and so on. Although many parts such as seeding and soil suppression technology are optimizing gradually, research filling seeds are still rare (*Liu et al., 2022; Lian et al., 2012; Lei et al., 2018; Liu et al., 2011*).

Filling seeds by manpower is still the main stream in the current plot breeding settings. For the various plot and many types of experimental seeds, human operator cannot keep up to the machine automation. Seeding efficiency is significantly reduced due to interruptions required for manual seed refilling (*Shi et al., 2020; Liu et al., 2019; Liu et al., 2019*). Meanwhile, multi-row plot seeders still have many problems, such as poor seed dispersion, low precision, unstable performance at different operating speeds, complex structure, and difficult maintenance (*Liu et al., 2019; Wang et al., 2016; Li et al., 2009*).

In this work, in order to improve seed filling efficiency, decrease the seed damage rate, reduce the operator working load and enhance the mechanization level, an automatic seed filling device for a plot seeder used in soybean breeding was designed, taking into account soybean agronomic requirements and seed characteristics. The device mainly consists of two parts: a mechanical system and an electrical control system. The mechanical system includes components such as the seed cup, seed disc, base, and supporting bracket. Based on an analysis of the soybean seed filling process, the key factors influencing the seed cup structure design were identified, and a parameter analysis of these factors was carried out. As a result, the forward speed of the seeder and the rotational speed of the seed disc were selected as the test factors, while the qualification seed filling rate was chosen as the evaluation indicator. A quadratic regression orthogonal rotation design was conducted to determine the optimal combination of these factors. Finally, field experiments were performed to evaluate and verify the working quality, design rationality, and reliability of the device.

MATERIALS AND METHODS

1. Structure Design and Working Principle

1.1 Holistic Structure Design

The soybean plot seeder is mainly composed of the turntable seed filling device, the seeding device, battery pack part, driving motors, control box and structure frame. The three-dimensional diagram of the holistic structure design can be shown in Fig.1. The main technical parameters such as external dimensions, the ground clearance, structural quality, working row, motor power and so on are shown in Table.1.

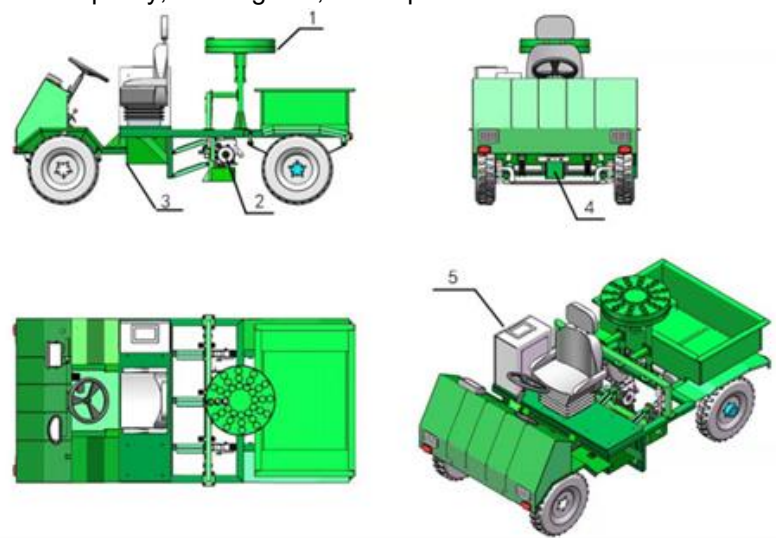


Fig. 1 - Diagram of the Soybean Plot Seeder Design

1. Turntable seed filling device; 2. Seeding device; 3. Battery pack part; 4. Driving motors; 5. Control box

Table 1

Main Technical Parameters				
Item	Unit	Value		
Dimensions (L*W*H)	mm	2400*1350*1000		
Ground Clearance	mm	300		
Structure Quality	kg	450		
Row Number	row	3		
Motor Power	kW	3		
Forward Maximum Forward Speed	km/h	8		
Backward Maximum Forward Speed	km/h	3		

1.2. Working Principle

The structure design diagram of the seeding device can be shown in Figure. 2.

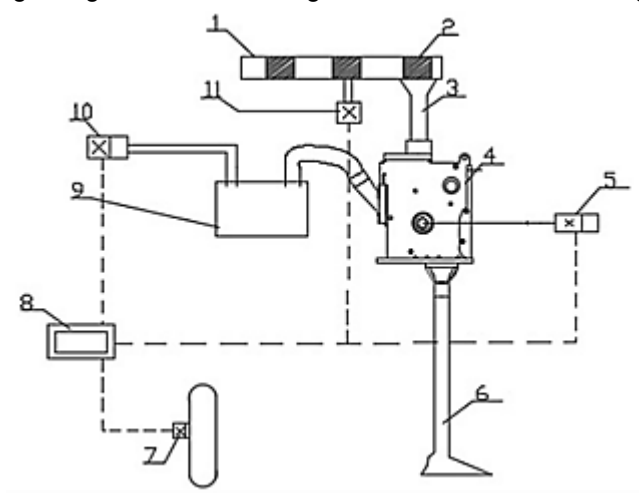


Fig. 2 - Diagram of the Seeding Device Structure Design

1. Seed filling device; 2. Seed cup; 3. Seeding pipe; 4. Seed box; 5. Stepper motor (seeding unit); 6. Seed boot; 7. Speed sensor; 8. PLC; 9. Seed recollection box; 10. Seed cleaning fan; 11. Stepper motor (filling disc)

The seeding device consists of an automatic filling system, a seeding system, and an automatic cleaning system. When the plot seeder reaches the border of the plot, the automatic filling system receives a signal to move the seed cup to the predetermined position. Then, the opening part of the seed cup is released, allowing the seeds to fall into the seeding box of the seeder through the seeding pipes. When the plot seeder begins operation, the encoder on the wheel transmits the forward speed signal to the PLC. Based on the PLC calculations, the rotational speed of the seeding device motor is adjusted to match the forward speed and maintain the required row spacing, ensuring that the seeds continuously fall into the furrow opened by the seed boot. Once the entire seeding process is completed, the seed cleaning fan is activated to remove the residual seeds from the seeding box and transfer them into the seed recollection box. After the seed cleaning process is finished, the plot seeder proceeds to the next plot to continue operation.

2. Design of the Automatic Seed Filling Device

2.1. Material Characteristics

Soybean seed is a type of granular material, characterized by looseness, good separability, and relatively uniform shape and size. To design a rational seed cup and other structural components, and to simulate its movement process, it is essential to identify and measure the mechanical properties of soybean seeds.

2.1.1. Moisture Content

Moisture content represents the percentage of water mass within a seed sample. It is not only an important factor affecting seed storage and germination, but also has a significant influence on many physical parameters of seeds. Currently, various methods are used to determine seed moisture content, including pulsed nuclear magnetic resonance, colour chromatography, Karl Fischer titration, capacitance measurement, and the oven-drying method (*Babić et al., 2013*). Considering both accuracy and operational simplicity, the oven-drying method was selected in this study to determine the moisture content of the soybean seed samples.

The process of measuring seed moisture content was carried out as follows:

- (1) The sample boxes were washed and dried to ensure they were clean and moisture-free. Each box was then weighed and labelled
- (2) A certain amount of soybean seeds (approximately 25-50 g) was weighed. The seeds were ground into powder using a pulverizer (with 70% passing through a 4.0 mm sieve). Two samples were randomly selected and placed into separate sample boxes for weighing.
- (3) The oven was preheated to 104-110 $^{\circ}$ C, and the temperature was stabilized at 105 ± 2 $^{\circ}$ C. The prepared samples were placed evenly on the upper tray of the oven, approximately 2.5 cm away from the thermometer bulb. The oven door was quickly closed, and the samples were dried for 1 hour.
- (4) After drying, the oven was opened, and the sample boxes were covered and allowed to cool to room temperature (approximately 30-45 minutes) before reweighing.

(5) Steps (3)–(4) were repeated until the difference between two consecutive weighing measurements was less than 0.2%. The moisture content of the soybean seeds was then calculated using the following formula:

$$\omega = \frac{M_2 - M_3}{M_2 - M_1} \times 100\% \tag{1}$$

In the formula:

 ω - Moisture content of the seeds;

 M_1 - Sample box mass (g);

 M_2 - Mass of sample box and sample before drying (g);

 M_3 - Mass of sample box and sample after drying (g).

The average moisture content of the soybean seeds (Wan Soybean 28), determined from three replicate measurements, is presented in Table 2.

Experimental Results of Soybean Seed Moisture Content

Table 2

Experimental Results of Soybean Seed Moisture Content						
	1		2		3	
	Ф	2	0	2	0	2
M1 (g)	25.41	25.42	25.41	25.41	25.42	25.41
M2 (g)	108.68	107.02	110.52	108.54	107.02	108.69
M3 (g)	101.35	99.89	103.14	101.22	99.84	101.36
Subgroup	0.088	0.087	0.087	0.088	0.088	0.088
Average	8.7	5%	8.7	5%	8.8	0%

2.1.2 Dimensions

During the design of the filling device, it is necessary to consider the sliding friction angle between the soybean seeds and contact materials. According to previous studies, the sliding friction angle of soybean seeds ranges from 19° to 25°. Since the plot seeder is a type of precision seeder, to prevent seed leakage, the slope of the seed cup cavity must be greater than the maximum friction angle of the seeds. Therefore, the seed cup cavity slope is selected as $\varphi = 30^\circ$. For current agricultural seeding requirements, a three-row plot soybean seeder must switch to a different seed type every 50 m of travel when the seed spacing is 10 cm, meaning that each row requires approximately 500 seeds per cycle. In practice, to ensure smooth operation of the filling device, at least two seeds should enter the seeding device simultaneously. Consequently, the output diameter of the seed cup must be greater than twice the average diameter of the seed. The statistical dimensions of the soybean seeds (Wan Soybean 28) were analysed to determine the equivalent diameter, following the method proposed by *Volkovas et al. (2006)*, as illustrated in Figure 3.

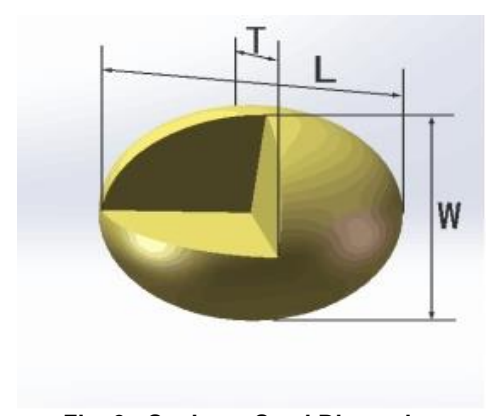


Fig. 3 - Soybean Seed Dimension

Equivalent diameter of the soybean seed D_P can be calculated as follows:

$$D_P = \sqrt[3]{LWT} \tag{2}$$

Sphericity of the soybean seed \emptyset can be calculated as follows:

$$\emptyset = \frac{D_P}{L} \times 100\% \tag{3}$$

As a result, the range of equivalent diameters and corresponding dimensions are presented in Table 3. The data follow a normal distribution, with approximately 87.6% of the soybean seeds falling within the 6.55 mm to 7.67 mm equivalent diameter range. The average sphericity of the seeds is 92.3%.

Soybean triaxial size and equivalent diameter

Table 3

ory bount triaxial one and organization attention				
L (mm)	W (mm)	T (mm)	Dp (mm)	
6.22~8.31	5.73~7.21	4.53~7.11	6.55~7.67	

2.1.3. Density

In this paper, the drainage method was used to measure the density of the soybean seed (*Fu et al., 2019*). The procedure is as follows:

- (1) Fill a graduated cylinder with a certain volume of water and record the initial volume V_0 .
- (2) Weigh a specific mass of soybean seeds (M), then carefully pour them into the cylinder (avoiding foam formation or splashing) and record the new volume V_1 .
- (3) Determine the displaced volume of the soybean seeds by calculating the difference between the two readings.
- (4) Calculate the density of the soybean seeds using Equation (4). Repeat the measurement three times and record the average value.

$$\rho = \frac{M}{V_1 - V_0} \tag{4}$$

 ρ - Density of the soybean seeds (g/cm³);

M - Mass of the soybean seeds (g);

V - Volume of the soybean seeds (cm 3).

The results are in Table. 4. The density of the tested soybean seeds was determined to be 1.35g/cm³.

Table 4

	The Experimental Result of the Soybean Density			
	1	2	3	
M (g)	64.53	66.26	66.94	
<i>V</i> (g)	47.81	49.69	49.22	
ρ (g/cm ³)	1.35	1.34	1.36	

2.2. Design of automatic filling device

Due to the limited volume of the seeder vehicle, the design of the filling device must ensure a compact structure and small overall size. In this study, the rotational disc plot seeder consists of mechanical components — such as the seed cup, seed disc, and base — and an electrical control system including the PLC, motor, and driver. The PLC, serving as the control core, receives the seeding instruction signal and activates the drive module to control the motor, which drives the rotation of the disc. When the disc rotates to the seed cup outlet, the seed cup switch fully opens, allowing the seeds to fall into the seeding device cavity, thereby completing the seed filling operation for one plot.

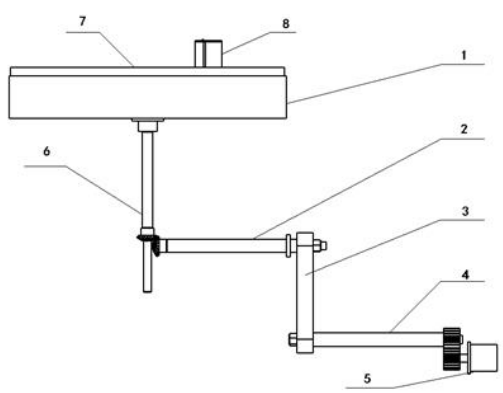


Fig. 4 - Diagram of the automatic seed filling device

1. Seed disc base; 2,3,4 Transmission pair; 5. Driving motor; 6. Rotating rod; 7. Seed disc; 8. Seed cup

2.2.1. Design of Seed Cup

Considering the sowing characteristics of soybeans in the HuangHuaiHai region of China, two soybean varieties (Wan23 and Wan28) were selected as test samples. The 1000-grain volume of the soybeans was measured using a volumetric cup, and the average value of multiple measurements was 310 mL. To meet the technical requirements of plot seeding, single-seed precision sowing was adopted, with a plant spacing of approximately 10 cm and a maximum sowing quantity of 500 seeds per plot. Considering extreme scenarios during the seeding process, the volume of the seed cup was determined to be no less than 170 mL.

As shown in Figure 5, the seed cup was designed as a cylindrical structure with a diameter of 40 mm, a height of 140 mm, and a calculated volume of 175.84 mL. Its bottom part was designed as a discharge port with an inclined conical surface. In addition, a seed baffle was installed at the discharge port of the seed cup, and a positioning boss was arranged on the outer edge of the seed cup to prevent free rotation.

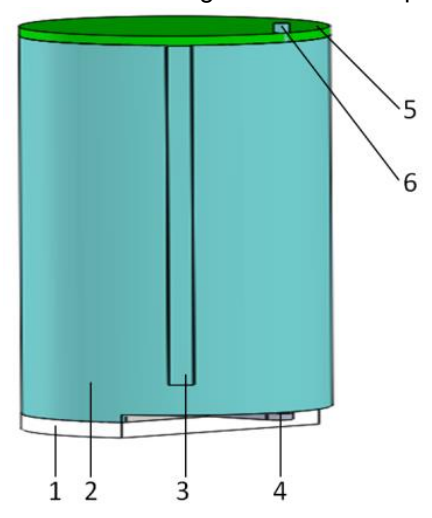


Fig. 5 - Diagram of seed cup 1. Bottom surface; 2.Main structure; 3.Locating boss; 4.Switch blade; 5.Cover; 6. Mounting column

To maximize seed discharge and improve seed-filling efficiency, the diameter of the discharge outlet was designed to be no less than 20 mm. For convenient fabrication and to maintain a compact shape and size, the discharge outlet was designed eccentrically relative to the seed inlet. Consequently, the outlet was positioned along the edge of the seed cup and evenly distributed to ensure that seeds entered the seed tube smoothly during the filling process, thereby preventing seed blockage or omission. The internal structure of the seed cup cavity is shown in Figure 6.

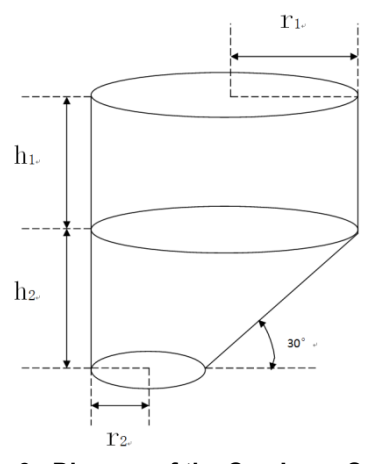


Fig. 6 - Diagram of the Cup Inner Cavity

The volume of the seed cup cavity V can be calculate using Equation (5) and must satisfy the conditions in Equation (6).

$$V = \pi(r_1)^2 \cdot h_1 + \frac{\pi}{3}(r_1^2 - r_2^2) \cdot h_2 \tag{5}$$

$$V = \pi(r_1)^2 \cdot h_1 + \frac{\pi}{3}(r_1^2 - r_2^2) \cdot h_2$$

$$\begin{cases} h_2 = 2 \cdot (r_1 - r_2) \cdot \tan \varphi \\ r_2 \ge 10 \\ r_1 > r_2 \end{cases}$$
(6)

where: *V*--volume of the seed cup cavity, ml;

 r_1 --inlet radius of the seed cup, mm;

 r_2 --outlet radius of the seed cup, mm;

 φ --gliding friction angle of the soybean seed;

 h_1 --upper height of the seed cup, mm;

 h_2 --lower height of the seed cup, mm.

By combining Equations (5) and (6), the relationships illustrated in Figures 7 and 8 were obtained using MATLAB curve fitting analysis.

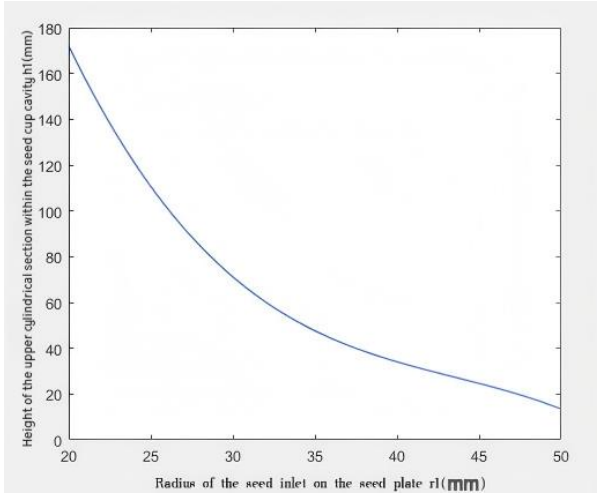


Fig. 7 - Relationship between the inlet radius r₁ and the outlet radius r₂

As shown in Figure 7, with the increase of r_I , the h_I gradually decreases. Within the range of Within the range of $45 \ge r_1 \ge 35$ (mm), the decrease in h_I becomes less pronounced, indicating that the influence of r_I on h_I gradually diminishes.

As shown in Figure 8, the effect of the r_2 on the h_I is minimal when the r_I remains constant. In comparison, the influence of r_I on h_I is the dominant factor. Therefore, r_I was set to 35 mm, r_2 to 15 mm, and h_I was designed to be greater than 50.8 mm. The upper structure of the seed cup is illustrated in Figure 9.

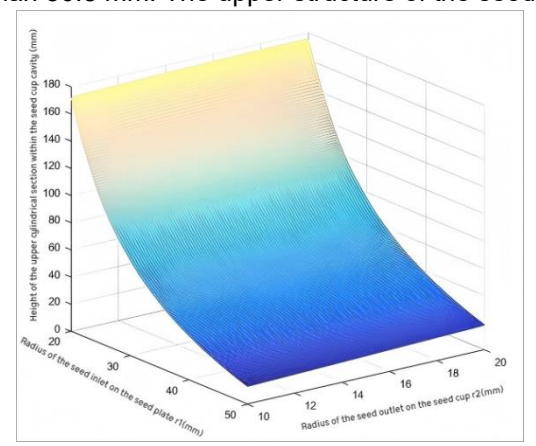


Fig. 8 - Relationship between r_1 , r_2 and h_1 of the seed cup

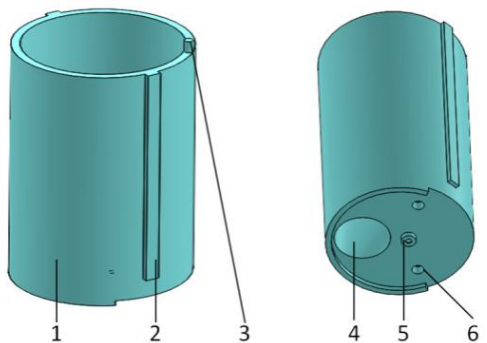


Fig. 9 - Upper Structure of the Seed Cup

1. Upper main structure; 2. Locating boss; 3. Mounting column; 4. Discharge opening; 5. Switch blade; 6. Locating hole

2.2.2. Design of the seed cup base

To achieve a compact structure, facilitate easy installation, and simplify switch blade replacement, the seed cup was designed with different radii for the seed inlet and outlet. In addition, adequate rotation space was reserved for the switch blade. The offset between the inlet and outlet ensures smooth seed entry during operation. The base of the seed cup consists of the bottom cover, switch blade, mounting screws, and other components, as illustrated in Figure 10.

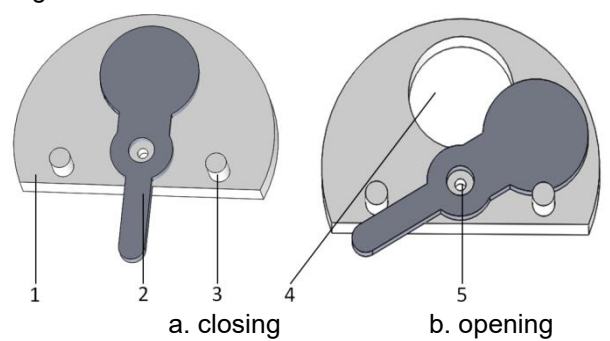


Fig. 10 - Bottom cover and switch blade situation

1.Bottom part; 2.Bottom cover; 3.Mounting column; 4.Output opening; 5.Screw hole

During operation, the switch blade gradually opens when the switch rod comes into contact with the switch column. When the seed disc rotates to the designated position and the outlet of the seed cup aligns with the discharge opening of the base, the seed cup fully opens, and the switch blade reaches its extreme position, as shown in Figure 10b. Subsequently, the motor pauses operation and waits for the next working cycle, thereby completing one automatic seed-filling process.

2.2.3 Design of the seed disc

The seed disc functions not only as a supporting component for the seed cups but also as a key mechanism for achieving automatic seed filling. In this study, the seed disc was designed with a diameter of 520 mm and a height of 100 mm. As shown in Figure 11, edge rims were machined at the bottom of the seed disc. During rotation, the switch columns on the base are positioned within these rims, preventing interference and providing a movement path for the opening of the seed cup switch blades. The rim diameter was designed as 470 mm, with a carving depth of 20 mm. Additionally, 36 mounting grooves for the seed cups are evenly distributed around the seed disc, each with a diameter of 200 mm. Every mounting groove includes internal positioning slots that provide support and alignment for the seed cups while preventing relative rotation between the seed disc and the seed cups. The drive shaft is powered by an electric motor. On the opposite end of the drive shaft, a hexagonal boss engages with the drive shaft hole of the seed disc, ensuring synchronous rotation between the motor and the seed disc. The diameter of the drive shaft was designed as 18 mm.

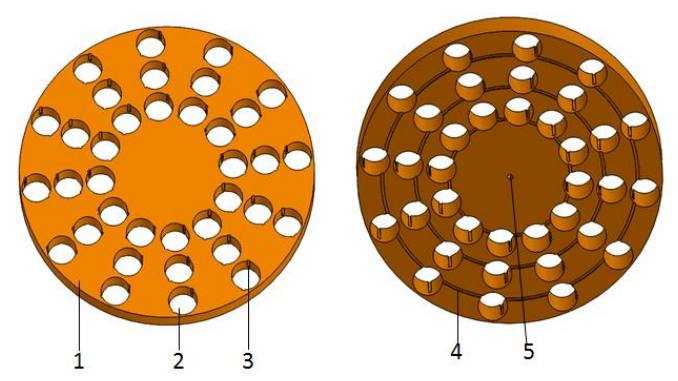


Fig. 11 - Overall structure of the Seed Disc

1. Seed disc; 2. Inner mounting groove of the seed cup; 3. Mounting groove of the seed cup; 4. Edge rim; 5. Drive shaft hole

2.2.4 Design of the outer tray of the seed disc

As shown in Figure 12, a DC stepping motor is mounted to provide rotational power. When the seed cup rotates together with the seed disc, the switch blade is obstructed by the switch column on the outer tray, creating relative motion between the switch blade and the seed cup. As a result, the outlet of the seed cup opens, allowing seeds to fall into the seeding cavity through the seeding pipe.

The outer tray of the seed disc was designed with a diameter of 522 mm. Three seed outlets on the tray are positioned along the same axis as the outlets of the seed cups, with the former being slightly larger to ensure smooth connection with the seeding pipes. The switch columns are distributed along a circular path of 485 mm in diameter on the outer tray. Each column has a diameter of 15 mm and a height of 16 mm.

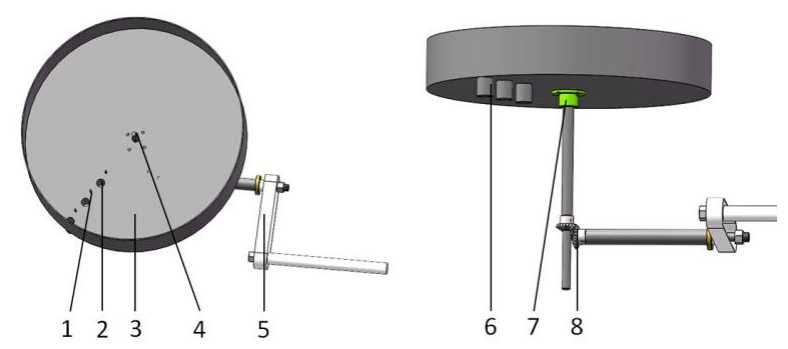


Fig. 12 - Structure of the outside tray of the seed disc

1.Switch column; 2. Tray outlet; 3.Tray main structure; 4. Drive shaft hole; 5. Drive system; 6. Mounting hole of tray outlet; 7.Shaft sleeve; 8. Bevel gear pair

2.3. Simulation analysis of the key components

The motion characteristics and connection methods of the geometric model of the key components were simulated and analysed using ADAMS software. In this section, the dynamic simulations illustrate different working conditions of the seed filling device.

2.3.1. Stress analysis of the seed disc

(1) Construction of the constraint model

The three-dimensional model of the device was created using SOLIDWORKS software. The model data were then exported in X_T format and imported into ADAMS software for simulation. Within ADAMS, constraint pairs, revolute pairs, and fixed pairs were established, as shown in Figure 13.

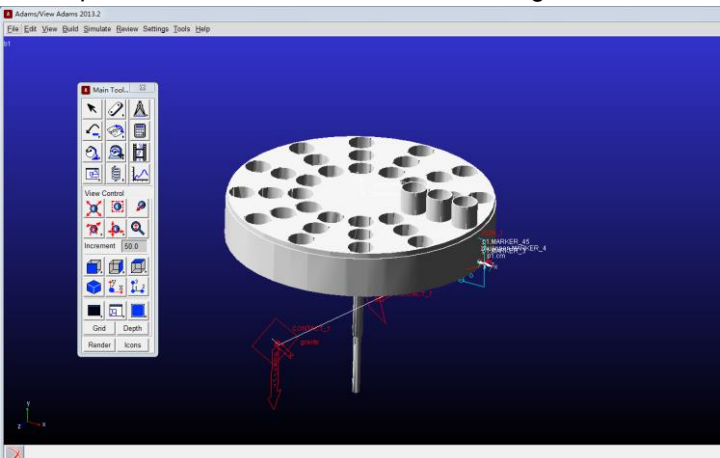


Fig. 13 - Constraint model in ADAMS

(2) Dynamic simulation of the model

First, the appropriate initial motion conditions were established, and the simulation parameters were configured according to the experimental setup. The step size and total simulation time were then determined. The simulation process of the device was performed after defining the specified motion laws.

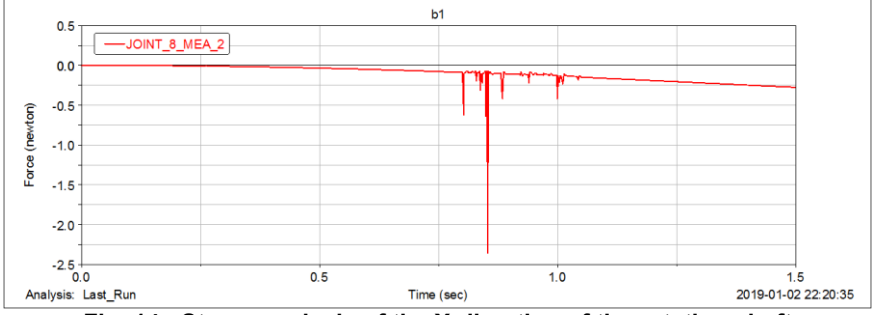


Fig. 14 - Stress analysis of the X-direction of the rotating shaft

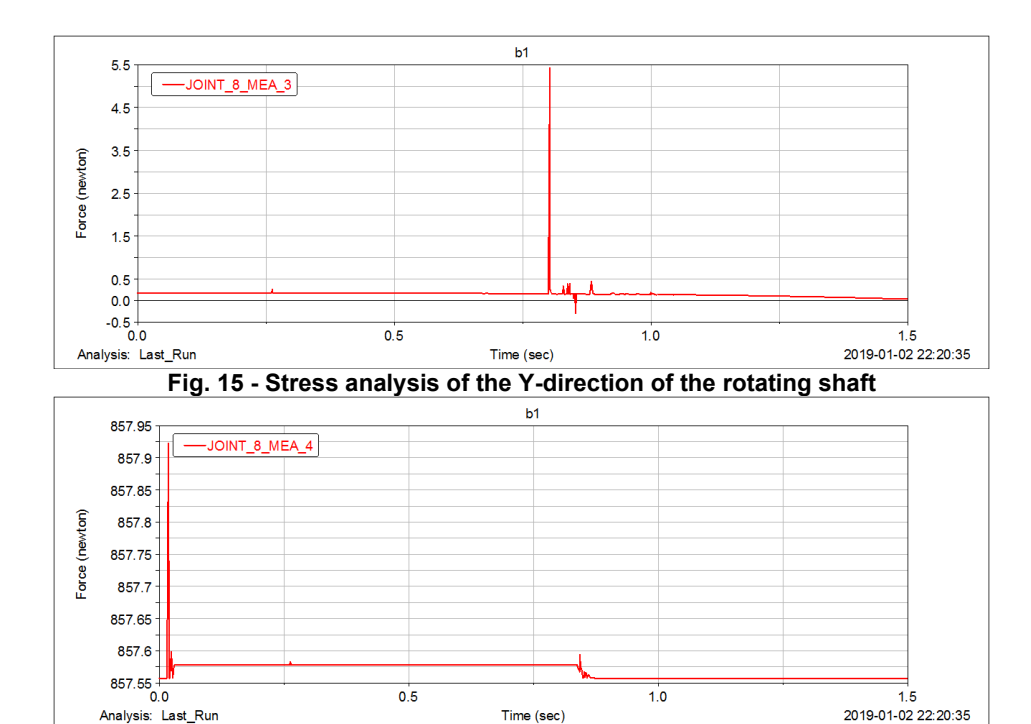


Fig. 16 - Stress analysis of the seed disc

As shown in Figures 14 and 15, the curves exhibit smooth trends at both ends but display noticeable fluctuations around 0.8 s. This phenomenon can be attributed to the change in the total mass of the seed disc, specifically due to seed discharge when the switch blade of the seed cup opens. In Figure 16, the initial segment of the curve shows intense fluctuations, followed by a transition to a stable trend. This indicates that the seed disc experiences high resistance at the start of operation, after which it maintains steady rotation. A slight fluctuation is also observed around 0.8 s, which is consistent with the stress analysis results in the X-and Y-directions. Overall, during the entire seed filling process, the operating stress of the system remains stable, and the stress variations caused by mass changes are highly transient.

2.3.2. Motion analysis of the switch blade of the seed cup

The switch blade of the seed cup is a critical component, as its motion directly affects the quality of seed discharge. The motion analysis of the switch blade was conducted to evaluate its operating performance, as described below.

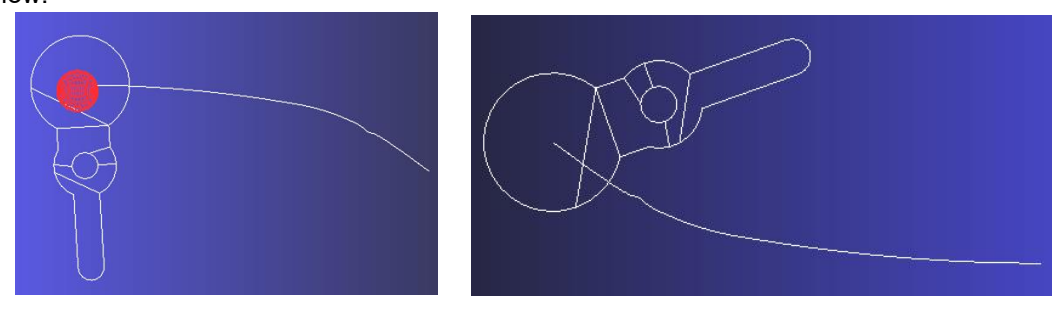


Fig. 17 - Motion track of the switch blade

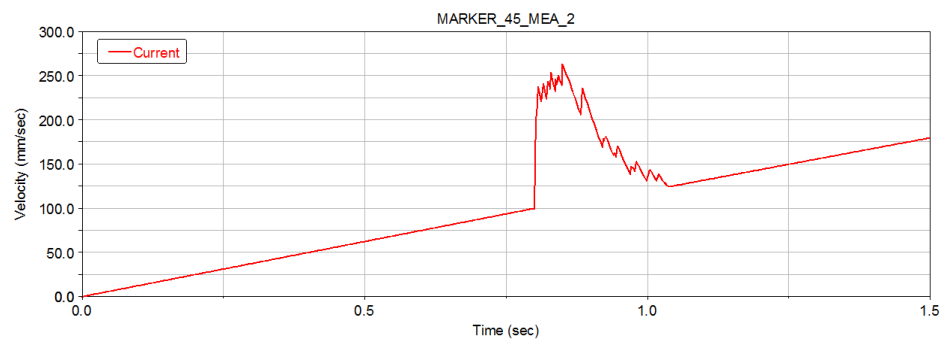


Fig. 18 - Speed curve of the switch blade

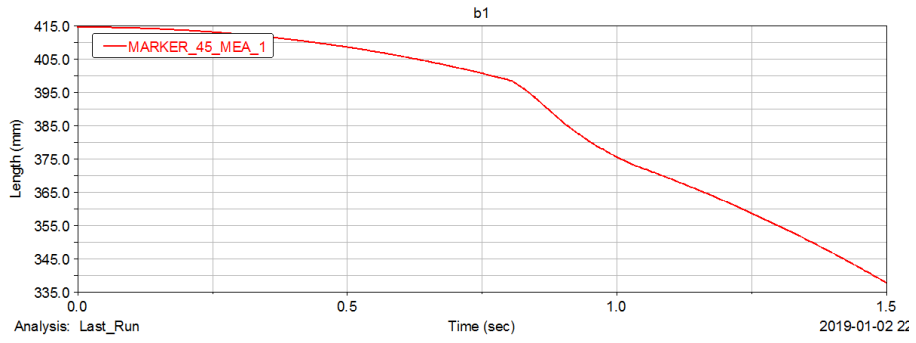


Fig. 19 - Displacement curve of the switch blade

As shown in Figure 17, the motion curve of the switch blade is smooth, indicating that it moves steadily and without obstruction during the opening process. In Figure 18, the switch blade rotates smoothly together with the seed disc. At approximately 0.8 s, the switch blade contacts the switch column, resulting in a temporary fluctuation in its speed. Afterward, the blade fully opens and continues to rotate synchronously with the seed disc as its speed gradually stabilizes. In Figure 19, the displacement curve of the switch blade remains smooth throughout the entire cycle, indicating that the blade's rotation around its fixed pivot point is steady, precise, and free of offset.

3 Experiment

3.1 Simulation analysis of the seed in the seed cup

EDEM is widely used simulation software based on the Discrete Element Method (DEM), commonly applied to analyse granular systems. In this study, the soybean granular system was modelled parametrically in EDEM by defining its mechanical features, material properties, and other relevant physical characteristics. Notably, the seed metering and seeding process was also simulated to visualize and evaluate seed movement and interaction within the seed cup.

3.1.1 Simulation parameter setting

Based on findings from previous studies, several parameters - including soybean particle properties, surface characteristics, particle-particle interaction properties, and particle-surface interaction properties - were determined, as listed in Tables 5 and 6 (*Wang et al.*, 2016).

Table 5

Item Property Value					
Soybean seed	Poisson's ratio	0.25			
	Shear Modulus (Pa)	1.04·106			
	Density(kg·m ⁻³)	1228			
Iron Surface	Poisson's ratio	0.3			
	Shear Modulus (Pa)	7·1010			
	Density(kg•m ⁻³)	7800			
	Recovery Coefficient	0.6			
Particle-Particle	Static Friction Coefficient	0.45			
	Dynamic Friction Coefficient	0.05			
Particle-Surface	Recovery Coefficient	0.6			
	Static Friction Coefficient	0.3			
	Dynamic Friction Coefficient	0.01			

Table 6

Particles parameters setting				
Property Value				
Particle length (mm)	7.667			
Particle width (mm)	7.582			
Particle height (mm)	6.945			
Surface 1 (X, Y, Z)	(0,-0.35,0)			
Surface 2 (X, Y, Z)	(0,0.35,0)			
Surface 3 (X, Y, Z)	(0,0,1.05)			
Surface 4 (X, Y, Z)	(0,0,-1.05)			

3.1.2. Definition of aggregates and particle factory

The pre-built model of the seed filling device was imported into EDEM, where parameters such as shaft rotational speed, virtual surfaces, and other simulation conditions were defined. The particle factory was configured using the dynamic generation mode, and the number of generated seeds was set to 120. After these parameters were established, the simulation was executed.

3.1.3. Simulation analysis

As shown in Figure 20, when the seed cup reaches the predetermined position, the switch blade opens, allowing the seeds to fall uniformly, completing the seeding process within the specified time of 12 s without any seed stagnation. As illustrated in Figure 21, the seeds begin to fall after a transport time of approximately 8 s. Each individual seed requires about 1 s to reach a maximum falling speed of 3 m/s, and after an additional 1 s, the seed is fully delivered into the seeding device. Therefore, the seeding process for a single seed is completed within 2 s. These simulation results confirm that the designed automatic seed-filling device effectively meets the predetermined performance requirements.

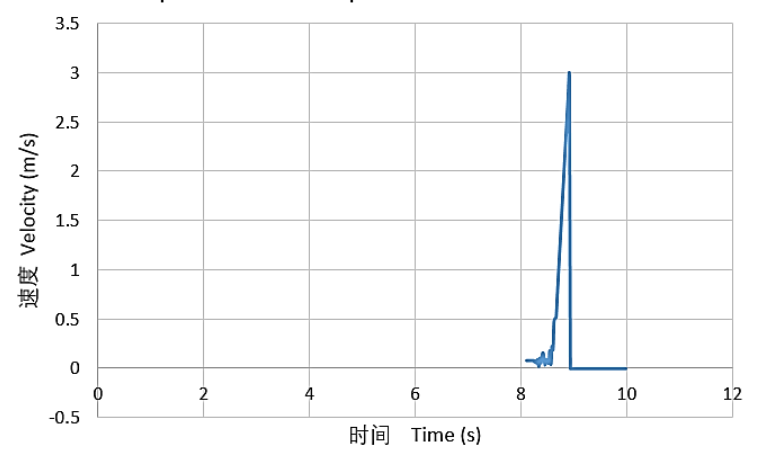


Fig. 20 - Seeding Process Simulation



Fig. 21 - Simulation of the seeding process for a single seed

3.2 Field Experiment

3.2.1 Experiment conditions

The test seeder used in this study was an electric soybean plot seeder prototype (*Wang et al., 2019*). The field experiments were conducted at the standard agricultural test field in Wuzhi County, provided by Rongda Technology Co., Ltd., China. The weather conditions, including temperature and humidity, met the requirements for field testing specified in GB/T 6973–2005 and JB/T 10293–2013. For the laboratory bench tests, the Wan 23 soybean variety was selected as the test specimen. Its 100-grain weight was approximately 23 g, with a moisture content below 12%, a Poisson's ratio of 0.413, and a shear modulus of 45.56 MPa. The seed cups were classified into 12 types, corresponding to weights of 20 g, 28 g, 36 g, 44 g, 52 g, 60 g, 68 g, 76 g, 84 g, 92 g, 100 g, and 108 g.

3.2.2 Experiment Method

3.2.2.1 Accuracy

During each seed-filling cycle, the outlet of the seed cup aligns accurately with the outlet of the outer tray on the seed disc. Both outlets open completely, with an offset error of less than 2 mm. In the seed-filling test, the filling device rotated 12 times, completing 12 groups of plot seedings. After each filling operation, the two outlets maintained high alignment accuracy, demonstrating the excellent performance of the automatic seed-filling mechanism. The total offset qualification rate of the experiment was calculated using Equation (7):

$$A_1 = \frac{n_1}{N_1} \times 100\% \tag{7}$$

 A_1 --total offset qualification rate for each test, %;

 n_1 --number of instances where the total offset was less than the equivalent radius in each test;

 N_1 --test number.

3.2.2.2 Reliability

The seeding quality was evaluated based on the percentage of unbroken seeds remaining in the seed cup during the automatic seed-filling process.

The unbroken seed rate was calculated using Equation (8):

$$A_2 = (1 - \frac{m_2}{M_2}) \times 100\% \tag{8}$$

where: A₂—unbroken seed rate, %;

m₂—average mass of broken seeds in each group, g;

M₂—total seed mass in each group, g.

After completing the seed-filling process for each group, both the outlet offset error of the seed cup and the unbroken seed rate were recorded. Once all seed cups completed their seed-filling cycles, the accuracy and reliability of the system were evaluated. Each test was repeated five times, and the average values were calculated. The results are presented in Table 7.

Field test results of the seed-filling device

Table 7

Mana		Offset		Broken Seed	
Group (g)	Average	Qualification	Average value of	Qualification rate	
	(g) value (mm) rate (%)	rate (%)	broken seed	(%)	
1	20	1.21	99.72	0	100
2	28	1.23	99.71	0	100
3	36	1.26	99.67	0	100
4	44	1.25	99.61	0	100
5	52	1.33	99.57	0	100
6	60	1.32	99.49	0.81	96.76
7	68	1.35	99.51	0.83	97.17
8	76	1.37	99.44	1.21	96.18
9	84	1.38	99.38	1.24	96.46
10	92	1.41	99.31	1.35	96.48
11	100	1.39	99.13	1.42	96.59
12	108	1.42	98.78	1.46	96.76
Average		1.33	99.44	0.69	98.03

The qualification rate of the offset for the 12 seed cup groups ranged from 98.78% to 99.72%, while the unbroken seed filling rate ranged from 96.18% to 100%. These results indicate that the seed-filling device demonstrates high accuracy and excellent reliability, effectively meeting the performance requirements for soybean plot seeding.

4. Discussion

In this study, a novel automatic seed-filling system was designed, featuring an electric seed disc driven by a stepper motor. The newly developed seed cups, which rotate synchronously with the seed disc, are capable of completing seed filling for 12 plots in a single working cycle. This design significantly enhances operational efficiency and reduces the workload of operators.

The ADAMS software was used to simulate and analyse the seed disc and switch blade of the seed-filling device. Analysis of the motion trajectories and stress distribution confirmed that both components meet the virtual performance requirements. In addition, EDEM software was employed to simulate and analyse the seed behaviour inside the seed cups. The simulation results verified that the designed seed cups enable smooth and continuous seed discharge into the seeding device without clogging or interruption.

Based on the analysis of the test process and results of the automatic seed-filling device, the main shortcomings of the design are summarized as follows:

(1) Effect of working environment

The unevenness of the field surface causes the plot seeder to move according to terrain variations. These vibrations affect the switch blades of the seed cups, sometimes leading to sluggish opening. This delay in blade response can hinder the seed-filling process and occasionally result in seed leakage.

(2) Motor step loss

When the plot seeder operates on irregular ground, its centre of gravity becomes unstable, increasing the internal resistance within the transmission system. This heightened resistance can cause the stepper motor to lose steps, resulting in timing delays or incomplete seed filling.

(3) Operator proficiency

The proficiency of operators also influences seed-filling quality. Even when the automatic system functions properly, inadequate operator training or improper handling can still lead to inconsistent seed filling. Therefore, it is crucial to expand standardized operator training programs to enhance both the accuracy and consistency of seed-filling performance.

CONCLUSIONS

- (1) To address the challenges in soybean plot seeders such as the absence of automatic seed-filling systems, the high labour intensity of manual filling, and low operational efficiency and accuracy this study designed and analysed a novel automatic seed-filling system. The system, powered by a stepper motor and PLC-controlled, integrates custom-designed components including seed cups, a seed disc, and a seed tray. This configuration enables automatic seed filling for 12 plots in a single working cycle, achieving automation, precision, and convenience in what was previously a labour-intensive process.
- (2) The key components of the automatic seed-filling system were designed, modelled, and analysed in detail. Using EDEM software, the motion behaviour of soybean seeds inside the seed cups was simulated, confirming that the seed cup structure is both rational and effective for achieving efficient seeding. Furthermore, an electrical control system was developed to improve operational convenience. Field tests conducted with 12 batches of soybean seeds validated the system's performance: the minimum qualification rate for seed cup offset was 98.78%, and the minimum unbroken seed-filling rate reached 96.18%. These results confirm that the proposed automatic seed-filling system meets the performance requirements of soybean plot seeders, ensuring high precision, reliability, and stability during operation.

REFERENCES

- [1] Babi'c, L.; Radojèin, M.; Pavkov, I.; Babi'c, M.; Turan, J.; Zoranovi'c, M.; Staniši'c, S. (2013). Physical properties and compression loading behaviour of corn seed. *Int. Agrophysics*, 27, 119–126.
- [2] Chen, H.T.; Wang, H.F.; Wang, Y.C.; Shi, N.Y.; Wei, Z.P.; Dou, Y.K. (2020). Design and experiment of three-leaf type air-suction seed meter with automatic clear and replace seeds features for soybean plot test. Trans. *Chin. Soc. Agric. Mach.* 51, 75–85.
- [3] Dai F, Zhang F W, Gao A M, Han Z S. (2012). Optimization of key operating parameters in 4GX-100 type cropland plot wheat seed combine harvester. *Transactions of the CSAE*, 28(Supp.2): 53–58.
- [4] Fu, Q.; Fu, J.; Chen, Z.; Han, L.; Ren, L. (2019). Effect of impact parameters and moisture content on kernel loss during corn snapping. *Int. Agrophys.* 33, 493–502.
- [5] Geng, A.; Yang, J.; Zhang, Z.; Yang, Q.; Li, R. (2016). Influence factor analysis of mechanical damage on corn ear picking. *Trans. Chin. Soc. Agric. Eng.* 32, 56–62.
- [6] Ghafori, H.; Hemmat, A.; Borghaee, A.M.; Minaei, S. (2011). Physical properties and conveying characteristics of corn and barley seeds using a suction-type pneumatic conveying system. Afr. *J. Agric. Res.* 6, 5972–5977. https://doi.org/10.5897/AJAR11.1098.
- [7] GB/T 6973-2005; China National Standard. Testing Methods of Single Seed Drills (Precision Drills). Standardization Administration of the PR China and General Administration of Quality Supervision. *Inspection and Quarantine of the PR China*: Beijing, China, 2005.
- [8] JB/T 10293-2013; China Machinery Industry Standards. Specifications of Single Seed Drill. *China Machinery Industry Federation*: Beijing, China, 2013.
- [9] Huang, M.; Zou, Y. (2018). Integrating mechanization with agronomy and breeding to ensure food security in China. *Field Crops Res.* 224, 22–27. https://doi.org/10.1016/j.fcr.2018.05.001.

- [10] Kroulík, M.; Hula, J.; Rybka, A.; Honzík, I. (2016). Seed passage speed through short vertical delivery tubes at precise seeding. *Agron.Res.* 14, 442–449.
- [11] Li, Z.; Wang, D.; Liu, G.; Yang, M.; Wang, Z. (2009). Experimental study on sowing seeds by air-stream metering mechanism. *Trans. Chin. Soc. Agric. Eng.* 25, 89–93.
- [12] Liu, J.; Wang, Q.; Li, H.; He, J.; Lu, C.; Wang, C. (2020). Numerical Analysis and Experiment on Pneumatic Loss Characteristic of Pinhole-Tube Wheat Uniform Seeding Mechanism. *Trans. Chin. Soc. Agric. Mach.* 51, 29–37.
- [13] Liu, L.; Liu, D.Q.; Sun, Q.T.; Qian, K.; Jin, T.T.; Li, X.J. (2022). Design and test of automatic seeding device for chain seeding box type plot planter. *J. Agric. Mech. Res.* 44, 89–94, 100.
- [14] Lian, Z.G.; Wang, J.G.; Yang, Z.H.; Shang, S.Q. (2012). Development of plot-sowing mechanization in China. *Trans. CSAE*, 28, 140–145.
- [15] Lei, X.L.; Liao, Y.T.; Zhang, Q.S.; Wang, L.; Liao, Q.X. (2018). Numerical simulation of seed motion characteristics of distribution head for rapeseed and wheat. *Comput. Electron. Agr.* 150, 98–109.
- [16] Liu, S.G.; Shang, S.Q.; Yang, R.B.; Zheng, Y.N.; Zhao, J.L. (2011). Analysis of plot seeder development. *J. Agric. Mech. Res.* 33, 237–241.
- [17] Liu, J.; Wang, Q.; Li, H.; He, J.; Lu, C. (2019). Design and seed suction performance of pinhole-tube wheat precision seeding device. *Trans. Chin. Soc. Agric. Eng.* 35, 10–18.
- [18] Liu, C.L.; Wang, Y.L.; Du, X.; Song, J.N.; Wang, J.C.; Zhang, F.Y. (2019). Filling performance analysis and verification of cell-belt rice precision seed-metering based on friction and repeated filling principle. *Trans. CSAE*, 35, 29–36.
- [19] Panigrahi, S.S.; Singh, C.B.; Fielke, J. (2021). Strategies to mitigate dead-zones in on-farm stored grain silos fitted with aeration ducting modelled using computational fluid dynamics. *Biosyst. Eng.* 205, 93–104. https://doi.org/10.1016/j.biosystemseng.2021.02.013
- [20] Shi, S.; Liu, H.; Wei, G.; Zhou, J.; Jian, S.; Zhang, R. (2020). Optimization and Experiment of Pneumatic Seed Metering Device with Guided Assistant Filling Based on EDEM-CFD. *Trans. Chin. Soc. Agric. Mach.* 51, 54–66.
- [21] Volkovas, V.; Petkevi cius, S.; Špokas, L. (2006). Establishment of maize kernel elasticity on the basis of impact load. *Mechanika*, 6, 64–67.
- [22] Wang, Y.X.; Liang, Z.J.; Zhang, D.X.; Cui, T.; Shi, S.; Li, K.H.; Yang, L. (2016). Calibration method of contact characteristic parameters for corn seeds based on EDEM. *Trans. Chin. Soc. Agric. Eng.* 32, 36–42.
- [23] Wang, S. (2019). Research and Design of Electric Drive Soybean Plot Seeder Based on Automatic Seeding System. *Ph.D. Thesis, Henan Agricultural University*, Beijing, China, 28.
- [24] Yang, W. (2019) Research on Technology and Equipment of Precision Seeding in Maize Breeding. Chinese Academy of Agricultural Mechanization Sciences. Beijing, China.
- [25] Yang, W.; Fang, X.F.; Li, J.D.; Li, L.X. (2019). Design and experiment of air-suction precision seed meter with self-clearing seed chamber for corn plot test. *Trans. Chin. Soc. Agric. Mach.* 50, 64–73.
- [26] Zhu, M.; Chen, H.; Li, Y. (2015). Investigation and development analysis of seed industry mechanization in China. *Int. J. Agr. Biol. Eng.* 31, 1–7.